Understanding the impact of field-emitter characteristics on electron beam focusing in the VAPoR Time-of-Flight Mass Spectrometer

Adrian E. Southard
University Space Research Agency and NASA Goddard Space Flight Center
Greenbelt, U.S.A
Adrian.e.southard@nasa.gov

Stephanie A. Getty, Nicholas P. Costen, Gregory B. Hidrobo and Daniel P. Glavin
NASA Goddard Space Flight Center
Greenbelt, U.S.A.

***Abstract*—Simulations of field emission of electrons from an electron gun are used to determine the angular distribution of the emitted electron beam and the percentage of charge transmitted through the grid. The simulations are a first step towards understanding the spherical aberration present after focusing the electron beam. The effect of offset of the cathode with respect to the grid and the separation between cathode and grid on the angular distributions of emitted electrons and transmission of the grid are explored.**

Keywords- Electron gun, mass spectroscopy, computer simulation

I. INTRODUCTION

To maximize the mass resolution of the time-of-flight mass spectrometer (TOFMS) being developed for the VAPoR instrument (Volatile Analysis by Pyrolysis of Regolith)[1], a simulation of field-emission from its electron gun is undertaken. The electron gun cathode is composed of an array of carbon nanotube based pillars [4] pointed towards a hexagonal grid, which provides the extraction field to produce an electron beam. Pillar height and alignment to the grid are still a challenging part of the electron fabrication to be reported on separately. The focus of this study is to examine how the height of these pillars and their position relative to the grid affect the angular distribution of electrons transmitted through the grid. This distribution affects the electron beam spot size which determines the size of the ionization region and ultimately the ability of electrostatic lenses to spatially focus an ion packet at the detector[3]. In addition, the transmission efficiency of the grid will also be determined as this impacts the sensitivity of the TOFMS.

In the TOFMS, the electron beam spot size In previous work, our electron gun featured a narrow aperture that reduced the electron beam acceptance angle, which had the interesting consequence of reducing contributions from spherical aberration at the ionization volume of the ion source. With recent improvements to the hardware to eliminate the narrow aperture and increase ionization efficiency, however, we have found that the resulting spherical aberration is now an important consideration in determining the smallest spot size attainable with the beam at the image focus [2].

I. APPROACH

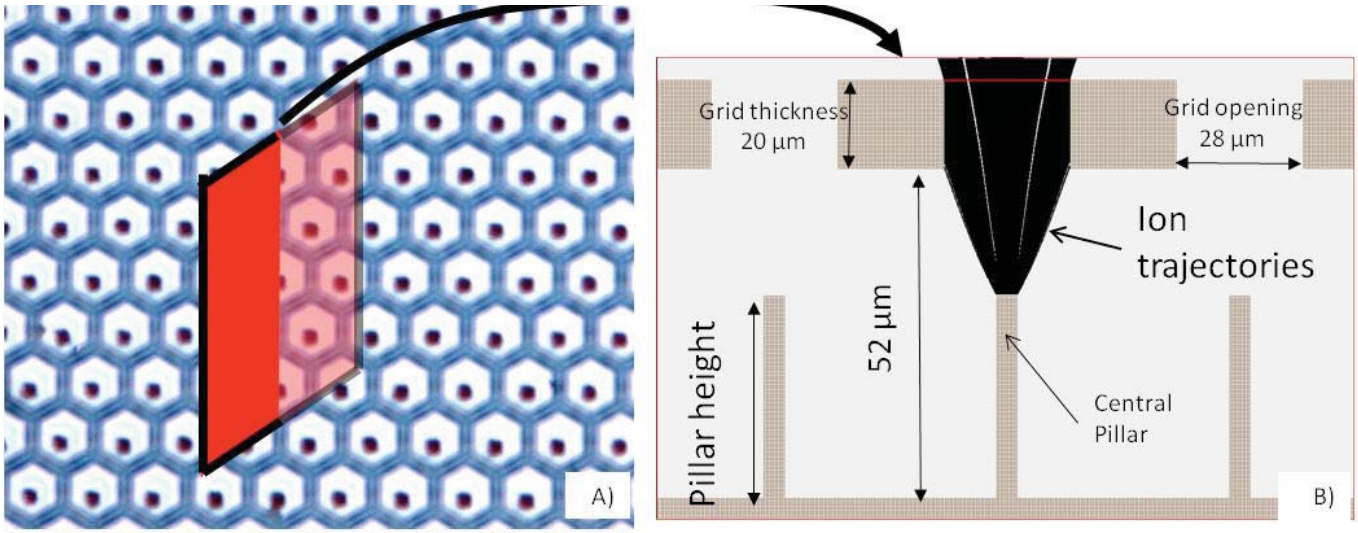

Figure 1(a) Contrast enhanced optical image of a section of one e-gun showing square carbon nanotube pillars below a hexagonal grid (top down view) with a red plane indicating the cross section shown in (b).

The angular and kinetic energy distributions of emitted electrons depend on the pillar geometry and its alignment to the grid which varies from electron gun to electron gun and even within the array of ~ 100,000 pillars and grid elements used in our emitter array. A top-down view of a section of one of the fabricated pillar arrays is shown in Fig. 1a. This particular emitter features square pillars and a hexagonal grid. A schematic of the cross-section of this array, indicated by the red plane in Fig. 1a is shown in Fig. 1b.

We explored the effects of pillar height and grid-pillar misalignment on the performance of the electron gun. A software package, SIMION, was used to determine trajectories of charged particles in the presence of electric and magnetic fields[5] for various emitter geometries. The emitter was simulated using dimensions that closely match as-fabricated emitters. The spacing between the surrounding substrate and the grid was held constant, as is the case in fabrication. Because major features in the emitter are on the one-micron scale, the model used a 0.25 μm/grid unit mesh. The model contained a representative sub-array of 7 pillars, each with 5 μm x 5 μm square cross section. These pillars are positioned below a commensurate array of hexagonal grid holes, each with a 28 μm opening along the diagonal. The pitch along the arm-chair direction of the lattice was 30 μm. The grid thickness used was 20 μm and the gap between the cathode substrate surrounding the pillars and the grid was 52 μm.

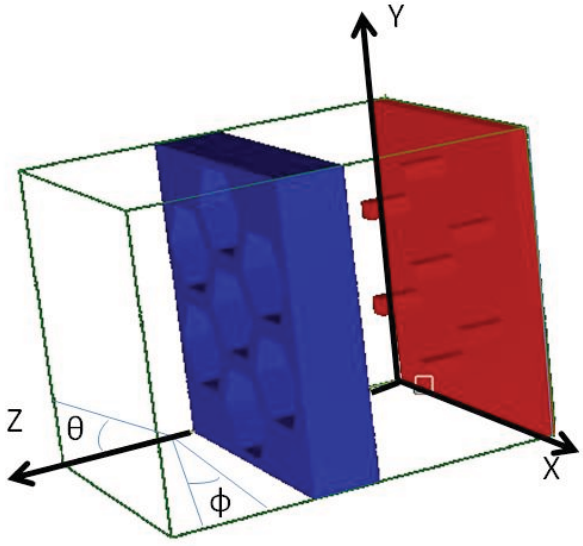

Figure 2 A three dimensional SIMION model of a section of the pillar-

As shown in Figure 2, the seven pillars are arranged in a hexagonal geometry. Although the electron emission was only simulated at the central pillar, the six pillar/grid elements on the perimeter were necessary to screen the effects of Neumann boundary conditions applied at the edge of the potential array. The model shown in Fig. 2 contains 13.5 μm-high pillars positioned directly below the center of the holes, i.e. a 0 μm pillar array offset along both the x and y axis. The models used to simulate various pillar heights and offsets in pillar positions with respect to the grid were based on the model shown in Fig. 2. In simulations of the emitted electron trajectories, 16 electrons were emitted per grid point, a total of 6561 electrons. These electrons were birthed at locations uniformly distributed at the top of the central pillar with zero kinetic energy and allowed to move in the field between the pillar array, at 0 V, and the grid, at 200 V. This potential difference is typical for electron gun operation. Because of the square pillar cross-section, the Fowler-Nordheim field enhancement factor is expected to vary across the top "surface" of the pillar. The resulting variation of emission current across the top of the pillar was accounted for by invoking a charge weighting factor, which is a value normally used to allow one particle to represent a cluster of ions or electrons. Here, it associates a weight to each simulated electron that can be chosen to be proportional to the Fowler-Nordheim emission current, I_{FN}:

$$CWF = I_{FN} = \alpha F^2 exp(-\beta/F) \quad (1)$$

where F is the electric field in V/grid unit (denoted V/gu), α depends on the work function and area of the emitting surface and β depends on the work function of the pillar and field enhancement due to individual carbon nanotubes extending above the pillar surface. Note that traditionally, β, accounts for any electric field enhancement beyond what is obtained with a parallel plate geometry; however, here field enhancement due to the pillar's shape modifies the local value of β and further enhancement due to nanoscale effects, e.g. pillars that protrude above the pillar's surface, are subsumed into the parameter β. For the sake of comparing various emitter geometries, α and β have been set equal to 1 V^2/gu^2 and 1 V/gu, respectively. This value for is representative of a pillar surface where individual carbon nanotubes are

emitting without screening one another and exhibit field enhancement factors of ~19,000. Note that field enhancement factors of individual multiwall carbon nanotubes up to 30,000 have been reported[6]. It must be noted, then, that the values produced in this study must be treated qualitatively; we will focus only on comparisons between model geometries, rather than making quantitative predictions of experimental field emission currents. The fine granularity in field emission properties due to the fact that the pillars comprise ~ 1000 individual carbon nanotubes is outside of the scope of this study. It is therefore assumed that the field computed here averages over nanoscale variations in the field due to field enhancement at the tips of carbon nanotubes.

II. Prepare Your Paper Before Styling

Within the geometry of the TOFMS, the ionization volume is described by the intersection of the electron beam and the ion acceptance into the instrument. Therefore, the width of the electron beam along the ion path has a direct influence on mass resolution. Since ions formed after electron ionization are extracted parallel to the y-axis, electrons emitted at small values of θ, the elevation angle, are ideal (Fig. 2). Thus, the following discussion will focus on how the pillar-grid geometry affects elevation angle distributions. A narrow electron distribution centered about $\theta = 0$ degrees is desirable for optimized TOFMS performance.

In Fig. 3, the y-axis is proportional to the amount of charge transmitted through elevation angles of 2 degrees, regardless of azimuthal angle ϕ, normalized by the total charge emitted, and plotted as a function of elevation angle.

An offset in position along the x-axis, denoted X offset in Fig. 3a leads to an almost symmetric distribution whose peak height is reduced almost uniformly as offset is increased. A slight asymmetry in the elevation distribution with no X nor Y offset is due to limitations in the potential refinement at the edges and corners of the pillars. Note that even with no offset, a small number of electrons are able to pass through all six of the grid holes surrounding the central one and this leads to small peaks in the spectrum at -12 and 14 degrees. A Y offset leads to a strongly asymmetric distribution (Fig. 3b), redistributing emission at 0 degrees to emission at 3 degrees. The case of a Y offset of 10 μm results from the beam exiting through four different grid holes.

Table 1 Effect of pillar array offset on the percentage of charge transmitted given a fixed pillar height of 13.5 μm

Pillar-Grid geometry configurations				
X offset (μm)	*Y offset (μm)*	*Pillar height (μm)*	*Charge transmitted (%)*	*Charge emitted (V^2/gu^2)*
0	0	13.5	70.0	90815
5	0	13.5	58.6	90580
10	0	13.5	49.2	90069
0	5	13.5	58.6	90645
0	10	13.5	52.8	90212
0	0	6.75	74.7	42016
0	0	27	70.0	218412

As pillar height is decreased, the elevation angle distribution becomes more sharply peaked, as shown in Figure 4. This is caused by a smaller variation of the field at and around the pillar surface. This is explainable due to the fact that a shorter pillar gives an electric field that approaches that of the constant field between two parallel plates.

In Table 1, a comparison of the amount of charge emitted and transmitted is given for each configuration simulated. Recall that the simulations are not sophisticated enough to predict the actual amount of charge physically emitted and that only comparisons between the different geometries can be made. The amount of charge transmitted is higher when X and Y offsets are zero or in the case of the shortest pillar. The amount of charge emitted is largest when the electric field is largest which for a constant applied voltage is when the gap between the pillar and grid is smallest.

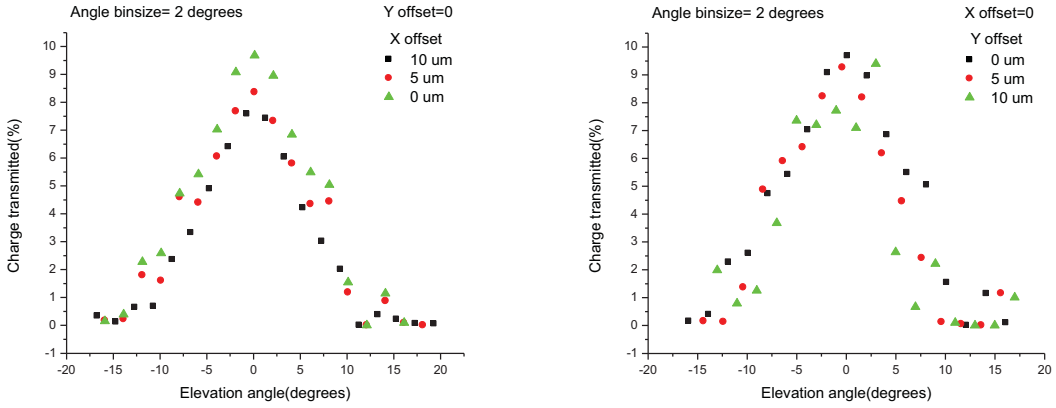

Figure 3 Impact of pillar array offset along the (a) x-axis and (b) y-axis on the elevation angle distribution.

III. SUMMARY

In simulated field emission from CNT pillars, enhanced electron emission at the vertices and edges of flat-top pillars produced a flatter elevation angle distribution and less overall charge transmission than would be the case if field this enhancement were ignored and the density of emitted

Work sponsored by the NASA Astrobiology Science and Technology for Instrument Development Program (07-ASTID07-0020).

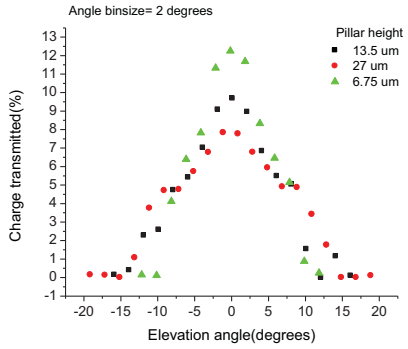

Figure 4 Impact of pillar height on the elevation angle distribution

electrons was independent of position along the pillar top. These edge and vertice effects would become more significant if field enhancement due to the large aspect ration of isolated carbon nanotubes was reduced by screening and would correspond to values of $\beta>1$.

The silicon beams making up the hexagonal grid are not thick enough to block emission through neighboring grid holes. This is especially evident when Y offsets are non-zero. A larger pitch with thicker beams could reduce this effect but at the cost of lower transmission of electrons through the grid. The effect of X offsets is to reduce the angular breadth of the beam at the expense of the percentage of charge transmitted. This effect is a result of the shape of the hexagonal holes making up the grid and would not present with a square grid. The shortest pillar height, 6.75 µm, showed a more pronounced peak in the elevation angle distribution and increased transmission of charge of ~5%; however, this corresponded to a reduction in emitted charge of more than 50% compared to the 13.5 µm pillar. In experiment, a larger bias voltage between the cathode and grid can compensate for reduced emission from a short pillar; however, this also increases power consumption due to both the emission current and any leakage currents between the cathode and emitter. The larger bias voltage may also necessitate the use of electronics especially rated for high voltages.

In conclusion, both pillar height and offset lead to a tradeoff between mass resolution and sensitivity. Determining the optimal geometry of the electron-gun will require examination of the impact of spherical aberration on the ability of electrostatic lenses to reduce the beam spot size.

IV. Acknowledgment

Thanks to David Manura for SIMION support and examples and Michael Collier for fruitful discussions.

References

[1] D. P. Glavin, C. Malespin, L. Inge, S. A. Getty, V. E. Holmes, E. Mumm, H. B. Franz, M. Noreiga, N. Dobson, A. E. Southard, and others, "Volatile Analysis by Pyrolysis of Regolith for Planetary Resource Exploration."

[2] M. Szilagyi, "Optimum design of electrostatic lenses," *Journal of Vacuum Science & Technology B: Microelectronics and Nanometer Structures*, vol. 6, no. 3, p. 953, May 1988.

[3] R. J. Cotter, *Time-of-flight mass spectrometry*. Wiley Online Library, 1994.

[4] S. A. Getty, T. T. King, R. A. Bis, H. H. Jones, F. Herrero, B. A. Lynch, P. Roman, and P. Mahaffy, "Performance of a carbon nanotube field emission electron gun," in *Proc. of SPIE Vol*, vol. 6556, p. 655618–1.

[5] Dahl D.A., "simion for the personal computer in reflection," *International Journal of Mass Spectrometry*, vol. 200, no. 1, pp. 3–25, 2000.

[6] J. L. Silan, D. L. Niemann, B. P. Ribaya, M. Rahman, M. Meyyappan, and C. V. Nguyen, "Carbon nanotube pillar arrays for achieving high emission current densities," *Applied Physics Letters*, vol. 95, no. 13, p. 133111–133111–3, Sep. 2009.

[7] M. Fransen, T. L. Van Rooy, and P. Kruit, "Field emission energy distributions from individual multiwalled carbon nanotubes," *Applied surface science*, vol. 146, no. 1–4, pp. 312–327, 1999.